Application of Large-Eddy Simulation to rotor/stator configurations

N. Gourdain[a], G. Wang[b], F. Duchaine[a] and L. Gicquel[a]

a. *CERFACS, CFD team, Toulouse, Fance*
b. *CERFACS, CFD team (now at University of Sherbrooke, Canada)*

Résumé :

Une meilleure compréhension des écoulements instationnaires est une étape nécessaire pour améliorer le dessin des composants des turbines à gaz. L'objet de ce travail est de tester la capacité de la Simulation aux Grandes Echelles (SGE) pour prédire l'écoulement turbulent dans un étage de turbomachine. Le premier cas test est la turbine haute-pression MT1. Le calcul est réalisé avec une version du code non-structuré AVBP. L'analyse des résultats montrent que les structures d'écoulement instationnaire, ainsi que les profils de pression, sont correctement estimés. La deuxième configuration est un étage de compression subsonique, investigué avec le code structuré elsA. Les performances ainsi que la structure de l'écoulement sont comparées aux mesures, montrant un bon accord entre les calculs et les essais.

Abstract :

A better understanding of unsteady flows is a necessary step towards a breakthrough in the design of gas turbine components. The objective of this work is to investigate the capability of Large-Eddy Simulation (LES) to predict the turbulent flow in rotor/stator configurations. The first application deals with the use of the unstructured solver AVBP for a high-pressure turbine. The analysis of results shows that major unsteady flow structures as well as statistics of pressure profiles are correctly estimated. The second application relies on the use of the structured code elsA. The configuration is an axial single-stage compressor. Compressor performance and flow features are compared with experiments, showing a good agreement.

Mots clefs : turbomachine, LES, turbulence

1 Introduction

The design of efficient gas turbines requires a better prediction of the components performance and understanding of unsteady flows. Among all components, the compressor and the turbine remain two critical part of a gas turbine.

Complementary to experimental investigations, the numerical simulation of flows, commonly referred to as Computational Fluid Dynamics (CFD), is a promising way to investigate such complex flows. While the Reynolds Averaged Navier-Stokes (RANS) model is the most common method, it has shown severe limitations due to turbulence modeling hypothesis. In that context, LES appears as a promising method to improve the reliability of flow solver predictions for a wide range of turbomachinery problems, such as off-design operating conditions [5, 9] and heat transfer [2, 4].

This paper proposes thus to report investigations based on LES. The paper is organized in two parts : the first one deals with the use an unstructured flow solver to compute the flow in a high-pressure turbine stage and the second one focuses on the simulation with a structured code in a low-pressure compressor stage.

For both applications, the governing equations are the filtered unsteady compressible Navier-Stokes equations for LES that describe the spatially filtered mass, momentum and energy conservation laws.

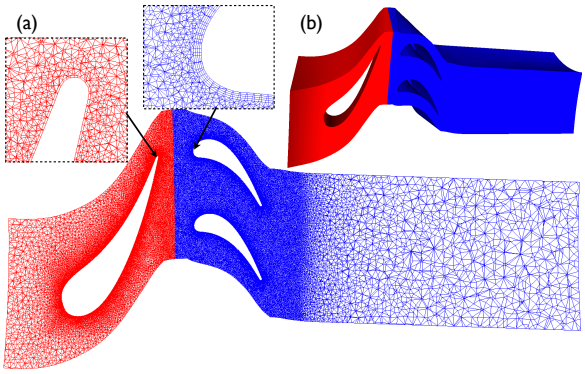

FIGURE 1 – View of the QinetiQ MT1 turbine : simulated domain with 1 scaled stator and 2 rotors : (a) mesh details and (b) computed flow passage.

2 Application to a high-pressure turbine

2.1 Numerical method

The equations are solved by the unstructured compressible LES solver, AVBP [12]. The rotor/stator coupling relies on a dynamic Domain Decomposition Methods (DDM). The exchange of information at the rotor/stator interface relies on external code coupling, through the parallel coupler OpenPALM [10]. More information about the method can be found in [13].

Characteristic boundary conditions (NSCBC) are used at inlet and outlet boundaries. The operating point is prescribed by targeting a mean static pressure value at the outlet. A classical logarithmic wall-law boundary condition is imposed on velocity to predict friction of solid walls. LES modeling relies on the standard Smagorinsky SGS model and the Lax-Wendroff scheme is used for convective fluxes. An explicit scheme is used for time marching, leading to a time step of $\Delta t = 0.5 \cdot 10^{-7}$ s which results into $126,000$ time steps to cover one full revolution of the machine. A full rotation costs about 4 K CPU hours.

2.2 Studied configuration

The MT1 turbine device is an un-shrouded, full-scale transonic high pressure research turbine established by EU projects TATEF 1 and TATEF 2 and tested in the Isentropic Light Piston Facility by QinetiQ [7]. It consists of 32 stator vanes and 60 rotor blades. At the considered operating condition, the rotational speed of the rotor is $9,500$ rpm, the mass flow rate is 17.4 kg/s and the isentropic Mach number at stator exit is 1.034 yielding a flow Reynolds number of $2.8 \cdot 10^6$ based on the stator chord and stator exit velocity.

To reduce the cost of the simulation, the computation deals with a rescaled geometry consisting in 1 scaled stator vane and 2 rotor blades in a 12° sector (Fig. 1). The stator vane is geometrically scaled by a small factor of 32/30 in order to establish spatial periodicity and maintain the solidity. Such scaling techniques are commonly used in unsteady rotor-stator simulations using both RANS approach [8, 6] or LES [9].

The unstructured hybrid meshes include a prismatic boundary layer mesh around the vane and blade surfaces while using tetrahedral cells away from these walls. The height of the prismatic layer is constructed based on a normalized wall distance so that $y^+ = 50 \sim 90$ around the blades with an aspect ratio of $\Delta x^+ = \Delta z^+ = 4\Delta y^+$. The resulting meshes finally consist of 13 millions hybrid prism/tetrahedric cells.

Results

Illustrations of normalized magnitude of the density gradient ($|\nabla\rho|/\rho$, corresponding to Schlieren image) are shown in Fig. 2 at different instants of the stator passing frequency. In this reference frame,

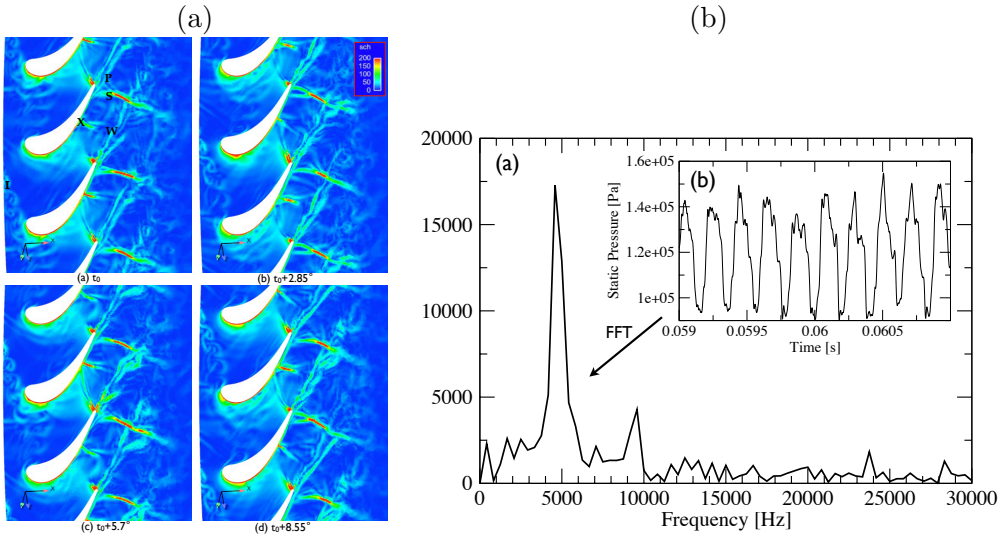

FIGURE 2 – (a) Sequential fields of $|\nabla\rho|/\rho$ ($H = 50\%$) in the relative frame of the rotor and (b) spectrum of a pressure signal at position **X**.

the incoming wake of the stator (denoted as **I** in Fig. 2) is periodically brushing the rotor passage. A shock (**S**) is found by the LES near the trailing edge of the blade. A second shock (noted **x**) is also captured on the suction side. Time series analysis for a probe positioned close to **x**, Fig. 2b, shows pressure variations between 0.95 and 1.45 bars. The frequency is close to $4,750$ Hz, and coincides with the stator passage frequency (in the frame of the rotor).

Results are compared to experimental data and RANS predictions reported in [11, 6]. Figure 3a & b shows the mean isentropic Mach number evolutions at two span heights (50% and 90%). All simulations are quite consistent with the experiments over the pressure side of both blades. On the suction side of the stator, Fig. 3a, close to the trailing edge ($x/C = 0.8$), LES results are in better agreements with experimental data than RANS results. Mean static pressure profiles at mid-span of the rotor blade are given in Fig. 3b. LES and RANS results are in reasonable agreement with experiments.

3 Application to a subsonic compressor

3.1 Numerical method

Equations are solved using the structured multiblock code *elsA* (see [1] for modeling capabilities). Convective fluxes are computed with a third-order upwind scheme. The subgrid scale model is the Wall-Adapting Local Eddy-Viscosity (WALE) model. The time-marching scheme is ensured with a second order Dual Time Stepping method. The inner loop relies on an implicit time integration scheme, based on a 2^{nd} order backward Euler scheme. The time step Δt is set to 3.95×10^{-7} (*i.e.* 24,000 time steps to describe one rotor rotation). At the outlet, a throttle condition is applied (coupled with a simplified radial equilibrium) to set the operating point. The minimum cell size at walls is set to 2 μm ($y^+ = 0.65$). A wall-resolved approach is chosen, leading to a total number of mesh points of 857.28×10^6 for the whole configuration (3 rotor blades and 4 stator vanes). With 1,024 computing core, the simulation of one rotor rotation requires 1,100,000 CPU hours.

3.2 Studied configuration

The test case is the CME2 compressor, originally investigated at the LEMFI laboratory [3] and now located at the Fluid Mechanics Institute of Lille (France). This axial compressor was designed by SNECMA in 1995 to provide representative unsteady rotor-stator interactions encountered in modern high-pressure compressors. This is a single-stage machine with 30 blades rotor and 40 vanes stator.

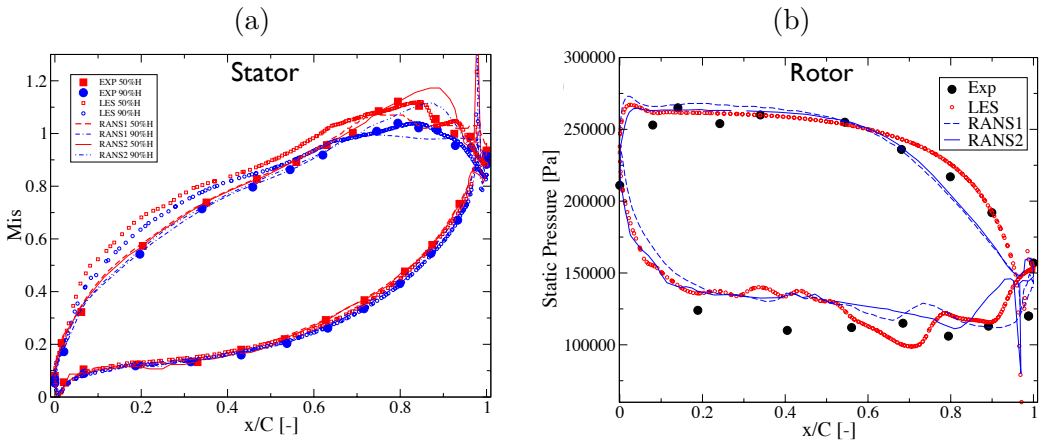

FIGURE 3 – Mean profile numerical predictions at different span-wise locations of the blades : (a) isentropic Mach number at 50% and 90% of the stator blade and (b) static pressure at 50% span of the rotor blade. results of RANS1from [11] and RANS2 from [6].

The outer tip radius is 0.275 m and the tip clearance represents 0.8% of the rotor span. The measured nominal rotation speed is $6,330 \pm 14$ rpm, which corresponds to a relative Mach number at tip of 0.534. At this rotation speed, the mean Reynolds number based on rotor chord and rotor exit velocity is close to $500,000$. At the nominal operating point, the mass flow Q is 10.50 ± 0.1 $kg.s^{-1}$, the total-to-total pressure ratio π is 1.15 and the isentropic efficiency η is 0.92.

3.3 Results

The comparison of URANS and LES results is shown in Fig. 4 (pressure ratio π) and Fig. 4(b) (efficiency η). The whole performance characteristic is described only with the URANS approach and LES are performed only at nominal conditions and for one off-design operating point. The shape of the experimental curve is well reproduced by the URANS approach, except close to the stall limit where the decrease of the pressure ratio is more pronounced in the simulation. At design operating conditions, URANS under-estimates the experimental pressure ratio by 0.3% while LES over-predicts it by 0.7%. Similarly, URANS under-estimates the nominal isentropic efficiency by 3.2% while LES over-predicts it by 3.0%.

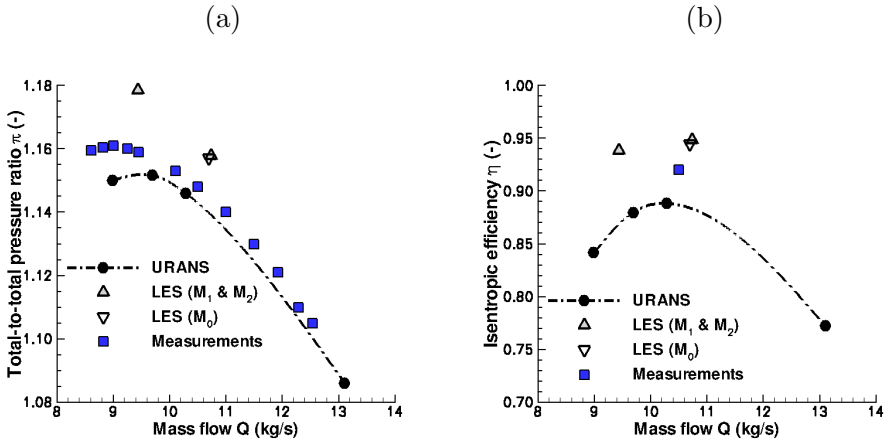

FIGURE 4 – Mean performance of the compressor : (a) pressure ratio and (b) efficiency.

An instantaneous flow field shaded with density gradient $grad\rho/\rho$ is shown in Fig. 5(a) close to the

rotor tip ($h/H = 90\%$). This flow field shows the complexity of the flow : boundary layer transition occurs both on rotor suction and pressure sides, the tip leakage flow (close to the rotor suction side) generates very high turbulent intensity, mixing with the rotor wakes and finally impacting the stator leading edge. A segregation effect is also observed in the stator, forcing turbulent flow patterns to migrate preferentially towards the pressure side. This picture indicates that very different scales exist in the flow (boundary layer vortices, inlet turbulence, wake vortices, tip leakage flow, etc.).

To show the impact of rotor wakes on the state of the stator boundary layer, some phase-average of velocity signals are performed inside the stator boundary layer, Fig. 5(b). It underlines the intermittent state of the boundary layer, especially from the leading edge ($S = 0mm$) to $S = 20mm$ (pressure side) and $S = 40mm$ (suction side). This plot also confirms the highest turbulent activity on the stator pressure side due to the accumulation of turbulent spots (segregation effect).

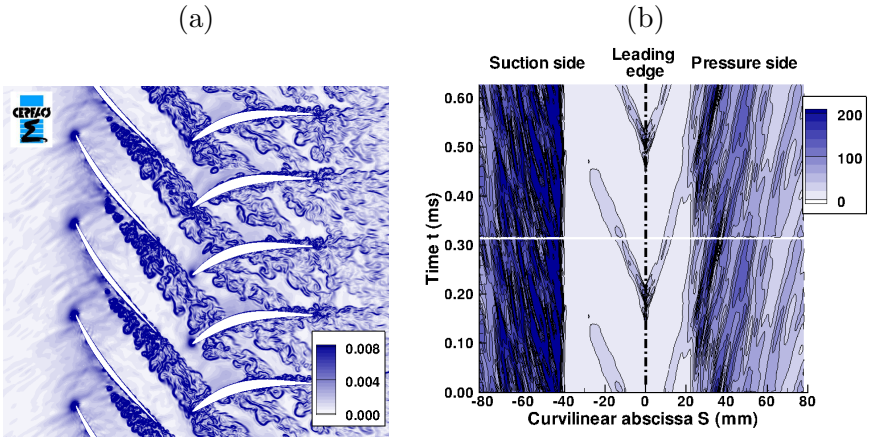

FIGURE 5 – Some LES results : (a) instantaneous flow field shaded with density gradient $grad\rho/\rho$ at $h/H = 90\%$ and (b) estimation of the boundary layer state in the stator : phase-averaged of velocity signals at $y^+ = 20$ (value is expressed as a turbulent kinetic energy in $m^2.s^{-2}$.

The evolution of the turbulent kinetic energy k is plot at $y^+ \approx 20$ in Fig. 6(a) (rotor) and Fig. 6(b) (stator). These results clearly underline that the transition does not occur at the leading edge as usually assumed in most simulations. In the rotor, the start of transition is observed at 40% of the chord on the suction side and 50% of the chord on the pressure side. The transition is triggered in the rotor by the adverse pressure gradient. The behavior in the stator is similar : a small peak of k is observed at the leading edge due to the impact of rotor wakes, then the turbulent kinetic energy vanishes until $S = 40$ mm on the suction side, where the adverse pressure gradient forces transition.

4 Conclusions

This paper relates the investigations done about the prediction of the turbulent compressible flow in axial turbomachine stages (one high-pressure turbine and one low-pressure compressor). Two applications have been performed, with two different codes and strategies (the first code is unstructured and the second one is structured). First, this contribution definitively demonstrates that LES is now accessible with modern computers, included for configurations at industrial conditions. Then, the short analysis of results reported in the paper shows that LES is a powerful approach to get information about complex flow physics and predict the performance of industrial configurations.

Acknowledgment

The author is also grateful to SAFRAN for authorization to publish results about turbine and compressor test cases. The author also thank ONERA for its support on the CFD code *elsA*. This work has benefited from CERFACS internal and GENCI-TGCC computing facilities (under the project gen6074). These supports were greatly acknowledged.

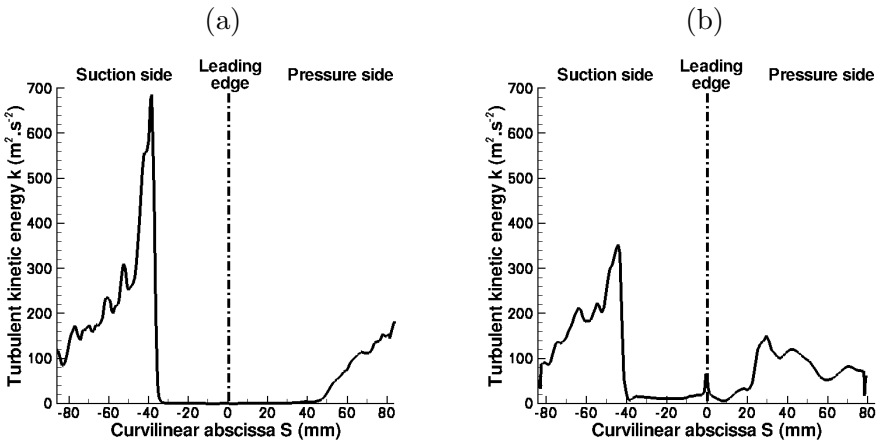

FIGURE 6 – Evolution of the turbulent kinetic energy at mid-span ($h/H = 50\%$) inside the boundary layer ($n^+ \approx 20$) : (a) rotor blade and (b) stator vane.

Références

[1] L. Cambier, S. Heib, and S. Plot. The onera elsa cfd software : input from research and feedback from industry. In *28th International Congress of the Aeronautical Sciences*, 2012.

[2] F. Duchaine, S. Mendez, F. Nicoud, A. Corpron, V. Moureau, and T. Poinsot. Coupling heat transfer solvers and large eddy simulations for combustion applications. *Int. J. of Heat and Fluid Flow*, 30 :1129–1141, 2009.

[3] T. M. Faure, G.-J. Michon, H. Miton, and Vassilieff. Laser doppler anemometry measurement in an axial compressor stage. *J. Propulsion and Power*, 17(3), 2001.

[4] N. Gourdain, L. Y. M. Gicquel, and E. Collado. Comparison of RANS and LES for prediction of wall heat transfer in a highly loaded turbine guide vane. *J. Propulsion and Power*, 28(2) :423–433, 2012.

[5] C. Hah. Large Eddy Simulation of transonic flow field in NASA rotor 37. Technical Report TM-2009-215627, NASA Glenn Research Center, 2009.

[6] Seyed Mohammad Hosseini, Florian Fruth, Damian M. Vogt, and Torsten H. Fransson. Effect of scaling of blade row sectors on the prediction of aerodynamic forcing in a highly-loaded transonic turbine stage. *ASME TURBO EXPO GT2011-45813*, 2011.

[7] A. D. Smith I. Qureshi, T. Povey and K. S. Chana. Effect of temperature nonuniformity on heat transfer in an unshrouded transonic hp turbine : An experimental and computaional investigation. *ASME Turbo Expo GT2010-22700*, 2010.

[8] Maria A. Mayorca, Jesus A. De Andrade, Damian M. Vogt, Hans Martensson, and Torsten H. Fransson. Effect of scaling of blade row sectors on the prediction of aerodynamic forcing in a highly-loaded transonic compressor stage. *ASME TURBO EXPO GT2009-59601*, 2009.

[9] W.A. McMullan and G.J. Page. Towards large eddy simulation of gas turbine compressors. *Progress in Aerospace Sciences*, 52(0) :30 – 47, 2012.

[10] A Piacentini, T Morel, A Thevenin, and F Duchaine. Open-palm an open source dynamic parallel coupler. In *Coupled Problems 2011*, 2011.

[11] Thomas Le Pichon. Modélisation aérodynamique et aérothermique externe des aubages de turbines axiales avec le code elsa. Technical report, TURBOMECA, 2008.

[12] T Schonfeld and M Rudgyardt. Steady and unsteady flow simulations using the hybrid flow solver avbp. *AIAA Journal*, 37 :1378–1385, 1999.

[13] G. Wang, D. Papadogiannis, F. Duchaine, N. Gourdain, and L. Y. M. Gicquel. Towards massively parallel Large Eddy Simulation of turbine stages. ASME Turbo Expo, 2013.